

A Model Predictive Control Strategy for improvement Performance in PV-Battery-Hydrogen DC Islanded Microgrid

Khalid Errakkas^{1,*}, *Mohammed Kissaoui*¹, *Rachid Lajouad*¹, *Abdelmounime El Magri*¹, *Youness Atifi*¹ and *Ahmed Khayat*¹

¹ EEIS Laboratory, ENSET Mohammedia, Hassan II University of Casablanca, Morocco

Abstract. This study introduces a new method for controlling Direct Current (DC) freestanding microgrids using Model Predictive Control (MPC). It focuses on integrating photovoltaic systems, battery storage, and hydrogen energy storage. The framework is designed to enhance operational efficiency and stability, especially in isolated or non-grid connected regions. The research uses simulation techniques and empirical data analysis to simulate various scenarios, revealing significant improvements in microgrid performance. The results show greater energy efficiency, and enhanced storage durability. The study suggests expanding the model to larger grid systems and adapting to different hybrid energy situations. This contributes to the development of more environmentally friendly and robust energy systems.

1 Introduction

The current energy sector is undergoing fast changes, shifting towards sustainability and efficiency. An essential aspect of this shift is incorporating renewable energy sources, particularly photovoltaics (PV), into the electricity system. Nevertheless, the sporadic characteristics of renewable energy sources, along with the growing need for dependable electricity provision, provide notable obstacles. Therefore, it is essential to create advanced control strategies in order to improve the performance and dependability of these systems [1].

Energy Management System (EMS) vary from basic to intricate multiparametric optimization algorithms. These advanced algorithms may factor in forecasts of electricity prices, load demands [2], weather conditions, operational costs, electricity market trends, and equipment degradation, among other aspects. Generally, EMS approaches can be categorized into two primary groups: heuristic-based methods and optimization-based methods.

Heuristic Methods: These are rule-based algorithms used in small microgrids, hybrid vehicles, and industrial plants. A common method is the Hysteresis Band Control (HBC), which operates Energy Storage Systems (ESSs) within certain thresholds based on their state of charge (SOC) [3]. For systems with multiple ESSs, the strategy involves multiple

* e-mail : khalid.errakkas@gmail.com

hysteresis bands, prioritizing more efficient systems [4]. The complexity of managing these systems increases with the number of rules and ESS types, like batteries, hydrogen, ultracapacitors, or flywheels.

Fuzzy Logic: This is used when managing complex heuristic rules becomes challenging [5]. Fuzzy logic, based on fuzzy sets theory, allows for varying degrees of membership rather than absolute binary conditions. This is useful for handling imprecise or incomplete data. Fuzzy Control (FC) is established using measurements and expert knowledge, and is adaptable to various microgrid applications, either alone or in combination with other controllers [6].

Optimization Problem in Microgrid Management: This involves minimizing a cost function under various constraints [7]. The aim is to determine optimal power levels for each Distributed Energy Resource (DER). Recent methods use single- or multi-objective optimization, considering operational costs, equipment lifetime, emissions, market prices, and hydrogen availability. Linear Programming (LP) is used for linear costs and constraints [8], while Quadratic Programming (QP) is for quadratic functions [9]. Nonlinear Programming (NLP) is required for nonlinear models or constraints, and for binary values [10-12], mixed-integer problems (MILP, MIQP, MINLP) are used, which are more complex and often require approximation techniques. Dynamic Programming (DP) is another method used, but it can be memory-intensive and challenging for large-scale problems [13].

This research study explores a novel method called Model Predictive Control (MPC) to enhance the efficiency of a DC islanded microgrid. The microgrid is a complex system that includes photovoltaics (PV), battery storage, and hydrogen energy components. The primary objective is to attain an ideal equilibrium between energy production, retention, and utilization, while guaranteeing stability and effectiveness.

The paper is organized into multiple essential sections:

Model Predictive Control (MPC): In this discussion, we explore the fundamental principles of MPC, its significance, and its benefits in effectively controlling intricate energy systems such as islanded microgrids.

Problem Formulation: This section clearly defines the specific difficulties and goals of the proposed Model Predictive Control (MPC) technique within the framework of a photovoltaic (PV), battery, and hydrogen-based microgrid.

Simulation Results and Discussion: This section focuses on presenting the outcomes of the simulations carried out to evaluate the effectiveness of the suggested Model Predictive Control (MPC) technique. The text conducts a thorough analysis of the enhancements in performance across many situations, examining the consequences and prospects for practical use.

2 Model Predictive Control

Model Predictive Control (MPC) is recognized as a leading advanced control technique in industrial applications, offering an optimal control solution for systems with constraints [14]. It leverages a system model to compute the control signal, aiming to minimize a specific cost function. The core idea of MPC involves selecting the optimal input from all possible input sequences over a predetermined future horizon, based on set criteria. Only the first input of this chosen sequence is executed on the system, and this process is cyclically updated with each new sampling period, adapting to new state information. This approach is known as the 'receding horizon' concept, depicted in figure 1.

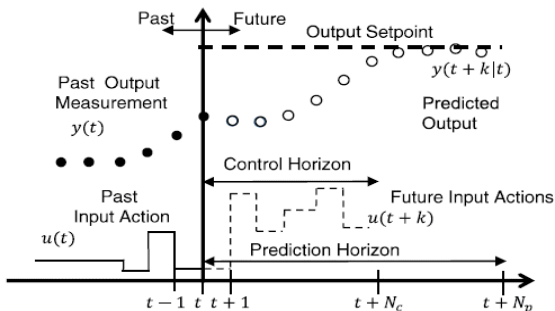


Fig. 1. Model Predictive Control strategy [14].

The process involves using a dynamic model to forecast the system's future output by analysing historical and current data, along with suggested optimal future control actions. These actions are determined by an optimizer that considers both the cost function and any existing constraints. The implementation of this strategy is carried out using a fundamental structure, as demonstrated in figure 2.

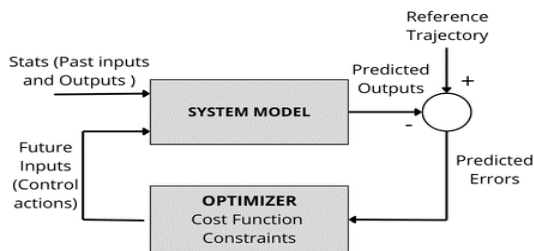


Fig. 2. MPC Structure [14].

2.1 Methodology

Multiple MPC's approaches are applicable for managing microgrids. Given the crucial role of storage in microgrids, their dynamic models are typically represented using state-space equations. In these models, the state variable $x(t)$ is aligned with the energy storage units' state of charge. This alignment makes state-space MPC a suitable method for microgrid control. State space models are effectively utilized to design predictive control problems. Additionally, such a formulation is adept at handling systems with multiple variables, a characteristic frequently seen in microgrids. For linear scenarios, specific equations are employed to describe the system's dynamics:

$$\begin{aligned} x(t + 1) &= Ax(t) + Bu(t) + B_d d(t) \\ y(t) &= Cx(t) \end{aligned} \tag{1}$$

In Single-Input Single-Output (SISO) systems, the state vector is denoted by $x(t)$, while $y(t)$ and $u(t)$ are scalar values. However, In Multiple Input Multiple Output (MIMO) systems, the situation becomes more intricate. Here, the input vector $u(t)$ has a dimensionality of m , and the output vector $y(t)$ has a dimensionality of n . Typically, the

output $y(t)$ corresponds directly to the state $x(t)$ in microgrids, indicating that the process is of the MIMO type. In this context, matrix C is equivalent to an identity matrix, reflecting the direct correspondence between the output and the state.

In the given model, B_d represents the matrix that quantifies the impact of disturbances $d(t)$ on the state variables [15].

2.2 Cost Function

The system dynamic model can be integrated into a cost function, which then becomes the focus of minimization efforts. Different Model Predictive Control (MPC) algorithms utilize various cost functions to derive the control law. Generally, the primary objective is to ensure that the future output $y(t)$ closely follows a specific reference signal $w(t)$ over the given horizon. This is achieved while also considering and penalizing the control effort $\Delta u(t)$ required to maintain this tracking. In the Single-Input Single-Output (SISO) scenario, the typical format of such an objective function would be presented accordingly.

$$J(N_p, N_c) = \sum_{j=1}^{N_p} \delta(j) [\hat{y}(t+j|t) - w(t+j)]^2 + \sum_{j=1}^{N_c} \lambda(j) [\Delta u(t+j-1)]^2 \quad (2)$$

In the given context, \hat{y} represents the predicted output. An additional component, which penalizes the control signal itself (rather than its increment), can also be integrated into the equation. The term N_p signifies the prediction horizon, while N_c , which is less than or equal to N_p , represents the control horizon. It's important to note that N_c doesn't necessarily have to match N_p in value.

The role of N_p is to define the limit of future time points at which the output is expected to follow the reference signal. The concept of the control horizon, denoted by N_c , involves the idea that after a certain time period (N_c , which is less than N_p), the proposed control signals are assumed to remain constant. This means that $u(t+j)$ will not vary for times beyond $j = N_c$

$$\Delta u(t+j-1) = 0 \quad j > N_c \quad (3)$$

This approach of keeping control signals constant after a certain time interval N_c can greatly decrease the number of decision variables involved. Consequently, this reduction simplifies the complexity of the problem at hand. In this framework, the coefficients $\delta(j)$ and $\lambda(j)$ are sequences that reflect the relative significance of error and control effort throughout the horizon. These sequences are instrumental in balancing the trade-off between closely tracking the desired output and minimizing the control effort required to achieve this tracking.

In the context of Multiple-Input Multiple-Output processes, both inputs and outputs are represented as vectors. As a result, the computation of costs in these systems typically involves the use of quadratic functions. These quadratic functions are adept at handling the multi-dimensional nature of the inputs and outputs, allowing for a comprehensive evaluation of the system's performance and the effectiveness of control efforts. This approach effectively captures the complexities and interactions inherent in MIMO systems, providing a robust framework for optimizing control strategies.

2.3 Constraints

In real scenarios, all systems operate within certain constraints. This is particularly true for generators and storage units in energy systems, which have defined operational limits and specific power rates. These constraints can arise from various factors including construction limitations, safety considerations, regulatory requirements, or environmental concerns.

For instance, in Energy Storage Systems (ESSs), there might be limits on storage levels, while power flows in lines, and maximum allowable temperatures and pressures are other common constraints. Therefore, incorporating these constraints into the optimization problem is essential for a realistic and effective control strategy. It ensures that the system not only performs optimally but also adheres to all necessary operational limits and standards

$$\begin{aligned}
 u_{min} &\leq u(t) \leq u_{max} && \forall t && (4) \\
 \Delta u_{min} &\leq u(t) - u(t - 1) \leq \Delta u_{max} && \forall t \\
 y_{min} &\leq y(t) \leq y_{max} && \forall t
 \end{aligned}$$

Indeed, constraints on the state variables $x(t)$, in a system can be integrated in a similar manner as output constraints. This is achieved by utilizing the same inequality expressions. To effectively apply these constraints to the state variables, the matrices C are set to be identity matrices. By doing so, the state variables $x(t)$, is directly linked to the output constraints. This approach simplifies the process of incorporating state constraints into the system, ensuring that the state variables adhere to the defined operational limits and conditions just as the output variables do.

3 Problem Formulation

This microgrid primarily relies on photovoltaic (PV) sources and hydrogen storage for its energy needs. Figure 3 illustrates a schematic of the microgrid, highlighting its key components. In typical operations, the energy generated by the microgrid doesn't always align with the demand [16].

To manage this imbalance, excess energy from photovoltaic (PV) can either be stored in a battery bank or converted into hydrogen through electrolysis. In times when PV power is not accessible, the system employs a fuel cell to transform the stored hydrogen into electricity, thus making up for the lack of generation.

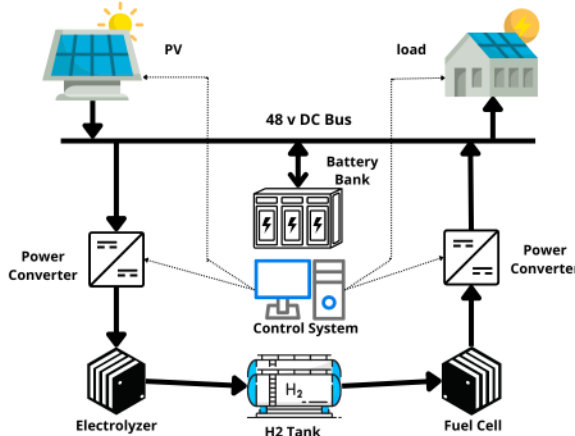


Fig. 3. Microgrid Scheme.

The integration of both electricity and hydrogen storage in this microgrid facilitates operational strategies across different time scales. The battery is capable of quickly absorbing or providing small amounts of energy to respond to rapid transient changes. In contrast, hydrogen storage is more suited for addressing larger fluctuations in energy demand or

supply. This hybrid storage approach enhances the flexibility and efficiency of the microgrid in managing energy.

In this photovoltaic-based DC microgrid, all the equipment, including the photovoltaic sources, battery bank, hydrogen storage, and fuel cell, are interconnected through a DC (Direct Current) bus. This setup is crucial for the efficient distribution and management of power within the microgrid.

To facilitate the transfer of power between these diverse components and the DC bus, appropriate power electronics are employed. These electronics are essential for converting and regulating voltages, ensuring compatibility between different elements of the system, and providing the means for efficient and safe energy transfer. This integration enables the microgrid to effectively manage the flow of electricity, both in storing excess energy and in supplying power when needed, maintaining a stable and reliable operation.

3.1 Control oriented Model

For designing the Model Predictive Control (MPC) of the photovoltaic-based DC microgrid, a control-oriented linear model is utilized, especially for managing the battery and hydrogen storage systems. In this context, the state-space model is an effective approach. The state vector in this model is defined as $x(t) = [SOC(t)LOH(t)]^T$. Here, SOC represents the State of Charge of the battery, indicating how much charge is currently stored in the battery relative to its total capacity. LOH stands for the Level of Hydrogen in the hydride tanks, which quantifies the amount of hydrogen available for energy production. To simplify the model and avoid the complexity of using binary variables, a fixed value for the battery's efficiency is assumed in this setup. This assumption means that the efficiency of the battery, which refers to how effectively it can convert stored energy into usable electrical power, is treated as a constant rather than a variable that changes with different operating conditions.

This simplification can make the model more manageable and easier to use for control purposes, although it might abstract away some of the nuances of real-world battery performance.

$$SOC(t + 1) = SOC(t) - \frac{\eta_{bat}Ts}{C_{max}} P_{bat}(t) \quad (5)$$

$$LOH(t + 1) = LOH(t) - \frac{\eta_{elz}Ts}{V_{max}} P_{elz}(t) - \frac{Ts}{\eta_{fc}V_{max}} P_{fc}(t) \quad (6)$$

P_{bat} , the power delivered by the battery which has a maximum capacity of C_{max} , and V_{max} , indicating the greatest volume of hydrogen storable in the tanks, are key variables. The controllable elements include the power interactions with the fuel cell (P_{fc}), the electrolyzer (P_{elz}), and the photovoltaic system (P_{pv}). As the battery is linked directly to the DC bus, it addresses any power imbalances, thereby necessitating P_{bat} to adjust in response to the remaining power activities on the DC bus.

$$P_{bat}(t) = P_{load}(t) + P_{elz}(t) - P_{fc}(t) - P_{pv}(t) \quad (7)$$

So, the storage equations, defining the measurable disturbance $d(t) = P_{pv}(t) - P_{load}(t)$ are:

$$SOC(t + 1) = SOC(t) - \frac{\eta_{bat}Ts}{C_{max}} (P_{elz}(t) - P_{fc}(t) - d(t)) \quad (8)$$

$$LOH(t + 1) = LOH(t) - \frac{\eta_{elz}Ts}{V_{max}} P_{elz}(t) - \frac{Ts}{\eta_{fc}V_{max}} P_{fc}(t) \quad (9)$$

3.2 Cost Function Formulation

The cost function may encompass terms that account for the various power values involved and can also impose penalties for deviations in stored energy from an optimal operational point. A cost function of the type described in equation (2) is adaptable for use in this specific case study.

$$\begin{aligned}
 J = \sum_{k=1}^{N_c} & \alpha_1 P_{fc}^2(t+k) + \alpha_2 P_{elz}^2(t+k) + \alpha_3 P_{bat}^2(t+k) + \beta_1 \Delta P_{fc}^2(t+k) \\
 & + \beta_2 \Delta P_{elz}^2(t+k) + \beta_3 \Delta P_{bat}^2(t+k) \\
 & + \sum_{k=1}^{N_p} \gamma_1 (SOC(t+k) - SOC_{ref})^2 \\
 & + \gamma_2 (LOH(t+k) - LOH_{ref})^2
 \end{aligned} \quad (10)$$

The cost function is structured such that the first three components measure the utilization of manipulated variables, and the subsequent three components penalize variations in their rates. The concluding elements are designed to keep the stored energy within a certain operational range. Here, a quadratic cost function is used, though a linear one could also be suitable. As the battery is connected directly to the DC bus, P_{bat} does not qualify as a manipulated variable and is therefore excluded from the u vector.

3.3 Physical and Operational Constraints

The microgrid's physical and operational constraints, including power limits and rates of the components, are integral to the optimization problem to enhance efficiency and lifespan. Specifically, the battery bank is constrained to operate within a specific SOC range to prevent overcharging and undercharging, which significantly impacts its usable cycles.

$$\begin{aligned}
 P_{elz}^{min} & \leq P_{elz}(t) \leq P_{elz}^{max} & \forall t & \quad (11) \\
 P_{fc}^{min} & \leq P_{fc}(t) \leq P_{fc}^{max} & \forall t & \\
 P_{pv}^{min} & \leq P_{pv}(t) \leq P_{pv}^{max} & \forall t & \\
 SOC^{min} & \leq SOC(t) \leq SOC^{max} & \forall t &
 \end{aligned}$$

4 Simulation Result and Discussion

In the microgrid configuration with hydrogen storage, the variables P_{fc} (power related to the fuel cell) and P_{elz} (power associated with the electrolyzer) are always positive and mutually exclusive, meaning they cannot be active simultaneously. Hence, they are considered complementary variables. To simplify the model and avoid incorporating this constraint directly, their effects can be combined into a single variable, $P_{H_2} = P_{fc} - P_{elz}$. This variable, P_{H_2} , represents the net hydrogen storage power. Consequently, the manipulated variable in the system is simplified to just $u(t) = P_{H_2}(t)$ this approximation is used in [17].

With these simplifications in place, for this case study the control-oriented model is designed based on a 5 second sampling interval (T_s). This choice of a short sampling interval is strategic, as it enables the system to rapidly react to abrupt fluctuations or disruptions in both energy demand and renewable energy generation. The specifics of this model, tailored to accommodate a 5 second sampling time, are as follows:

$$\begin{bmatrix} SOC(t + 1) \\ LOH(t + 1) \\ 7.8 \times 10^{-3} \\ 0 \end{bmatrix} = \begin{bmatrix} SOC(t) \\ LOH(t) \end{bmatrix} + \begin{bmatrix} 7.8 \times 10^{-3} & 7.8 \times 10^{-3} \\ -28.3 \times 10^{-3} & 0 \end{bmatrix} [P_{H_2}(t)] + \begin{bmatrix} 7.8 \times 10^{-3} \\ 0 \end{bmatrix} d(t) \tag{12}$$

As a result, the matrices that define the system's behaviour are as follows:

$$A = I, B = \begin{bmatrix} 7.8 & 7.8 \\ -28.3 & 0 \end{bmatrix} \times 10^{-3}, B_d = \begin{bmatrix} 7.8 \times 10^{-3} \\ 0 \end{bmatrix}, C = I \tag{13}$$

The cost function, with a minor modification from formula (8), incorporates P_{H_2} and excludes P_{bat} :

$$J = \sum_{k=1}^{N_c} \alpha_1 P_{H_2}^2(t+k) + \beta_1 \Delta P_{H_2}^2(t+k) + \sum_{k=1}^{N_p} \gamma_1 (SOC(t+k) - SOC_{ref})^2 + \gamma_2 (LOH(t+k) - LOH_{ref})^2 \tag{14}$$

Given that setpoint tracking isn't a significant concern, extremely low values ($\gamma_i = 10^{-8}$) have been selected for the corresponding weights. Other parameters include $\alpha_1 = 4.89 \times 10^{-3}$, $\beta_1 = 4$ and P_{bat} is not factored into the cost function. The horizons selected are $N_p = 12$ and $N_c = 2$.

To demonstrate the theoretical concepts, simulated microgrids were used to examine the controller's response to varying external conditions, such as changes in weather and demand. Two distinct scenarios were evaluated: a typical day, a sunny day and a cloudy day. The demand profile was based on a typical household's daily energy usage during a weekday, scaled to match the power levels of the microgrid [18]. Additionally, irradiance data was collected from a local meteorological station to inform the simulations. It's important to first validate the controller's performance in these simulations before implementing it in an actual plant.

Table 1 presented the technical specifications of the system components studied.

Table 1. Microgrid component's Power rate.

variable	Power (W)
PV	0-3000
Battery	0-1700
Fuel Cell	100-1200
Electrolyzer	100-900
Load	0-2500

Scenario 1: On a typical day, the generation profile fluctuates due to varying weather conditions. In the morning, solar irradiance gradually increases, allowing the battery to cover early demand until solar energy becomes sufficient. As solar power peaks at midday as shown in Figure 4, the battery fully charges, and excess energy is stored as hydrogen via the electrolyzer. In the afternoon, solar generation declines, and the battery supplements the energy supply. By evening, solar generation drops significantly, and the battery steps in to meet the deficit. At night, the battery continues to provide energy until it is depleted, after which the fuel cell generates energy from stored hydrogen. The Energy Management System (EMS) ensures a smooth transition between energy sources throughout the day. In figure 5 both the State of Charge (SOC) of the battery and the Level of Hydrogen (LOH) fluctuate within operational limits.

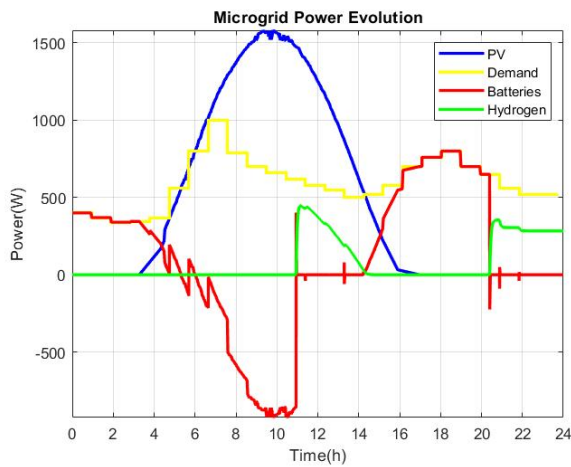


Fig. 4. Power Flow For a Typical Day.

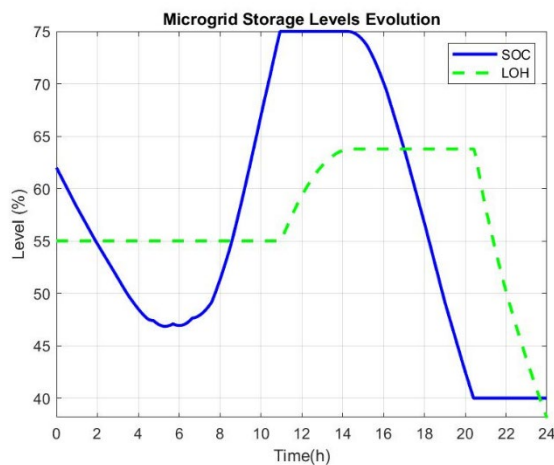


Fig. 5. Storage Level For a Typical Day.

Scenario 2: On sunny days, the generation profile is characterized by high solar irradiance, especially during midday, resulting in an excess of energy, while there's a deficit during the night. The Energy Management System (EMS) coordinates the battery and hydrogen storage units to meet demand. As depicted in Figure 6, the battery initially covers

The nighttime demand until solar generation creates an energy surplus. This surplus first charges the battery; any additional excess energy is then stored as hydrogen via the electrolyzer. During periods when photovoltaic (PV) generation falls short of demand, the battery steps in until it's depleted, after which the fuel cell begins to generate energy. It's notable in Figure 7 that the State of Charge (SOC) of the battery and the Level of Hydrogen (LOH) fluctuate almost freely within their operational bounds, as the weights in the cost function for reference tracking are kept low.

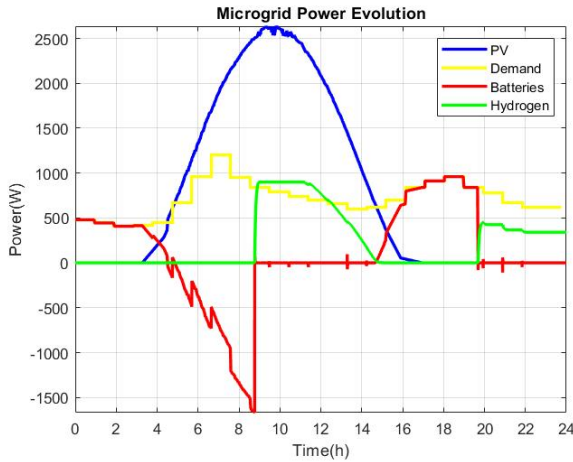


Fig. 6. Power Flow For a Sunny Day.

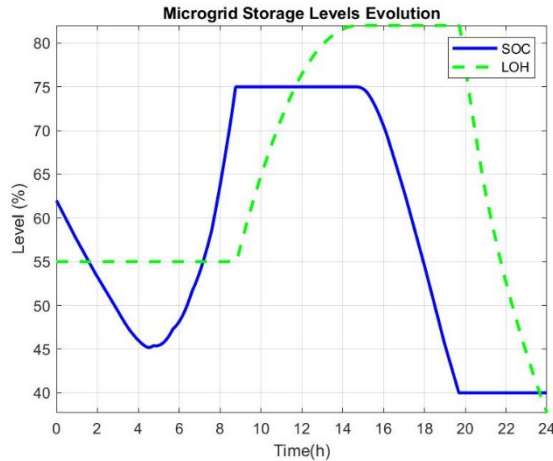


Fig. 7. Storage Level For a Sunny Day.

Scenario 3: On cloudy day, as illustrated in Figure 8, the photovoltaic (PV) generation is insufficient to meet demand for most of the day. To address this shortfall, the Energy Management System (EMS) relies on the available energy resources: the battery and the fuel cell. Initially, the EMS utilizes the battery, and later it seamlessly transitions to using the fuel cell.

Consequently, during the latter half of the day, when the battery reaches its minimum State of Charge (SOC) as shown in Figure 9, the load is sustained by the fuel cell. It's important to note that the electrolyzer remains inactive throughout this scenario, as there is no surplus energy available to be converted into hydrogen for storage.

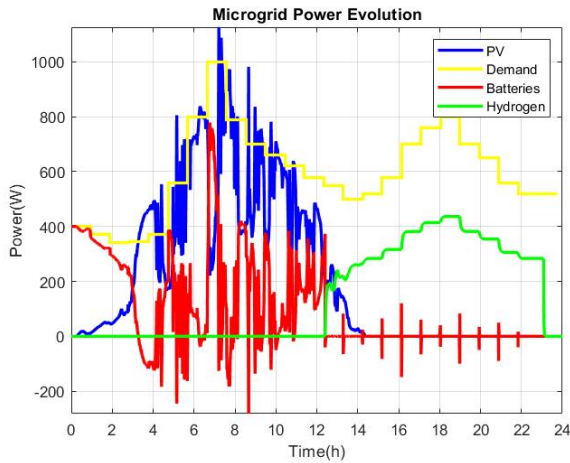


Fig. 8. Power Flow For a Cloudy Day.

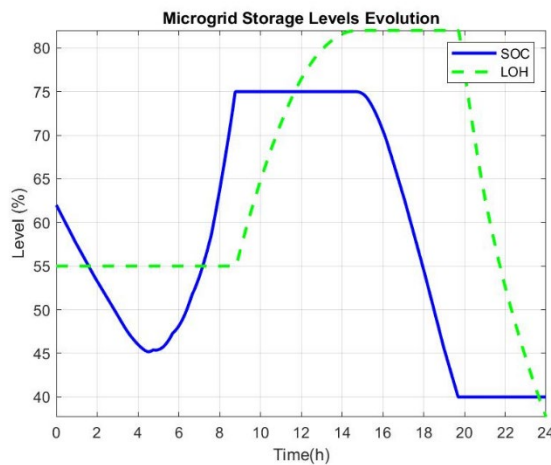


Fig. 9. Storage Level For a Cloudy Day.

Table 2 summarizes the SOC and LOH values at different time intervals for each figure based on the visual analysis of the plots.

Table 2. SOC and LOH level comparison for each scenario.

	Scenario 1	Scenario 2	Scenario 3
SOC (%) (Min-Max)	40-75	40-75	40-65
LOH (%) (Min-Max)	10-64	10-90	5-55

These simulations demonstrate how the MPC adapts to various scenarios, effectively managing power distribution among DERs while considering operational constraints and optimizing the established criteria $SOC^{max} \leq 75\%$ and $SOC^{min} \geq 40\%$ otherwise $LOH^{max} \leq 90\%$ and $LOH^{min} \geq 5\%$.

5 Conclusion

The strategic use of MPC contributes to a more balanced and efficient energy system. By proactively adjusting to fluctuations in energy supply and demand, MPC helps in maintaining optimal operating conditions for batteries, thereby preventing overcharging or deep discharging scenarios that can degrade battery health. This approach not only improves the overall efficiency of the microgrid but also ensures a more sustainable and cost-effective operation by prolonging battery life and reducing the need for frequent replacements.

The simulations highlight the versatility of Model Predictive Control (MPC) in diverse scenarios, this versatility is essential not only for adhering to operational constraints and optimizing based on predefined criteria, but also for enhancing the State of Health (SoH) of batteries. By intelligently managing charging and discharging cycles, MPC can reduce strain and extend the lifespan of batteries.

Although the current work emphasizes extending battery life through MPC, future studies could delve deeper into improving the accuracy of battery health estimation. Advanced battery models that account for temperature effects, aging, and usage patterns could be integrated into the MPC to further refine the control strategy, ensuring even better preservation of battery health and operational efficiency.

References

1. F. Dawood, G.M. Shafiullah, M. Anda, Stand-alone microgrid with 100% renewable energy: A case study with hybrid solar PV-battery-hydrogen, *Sustainability* **12**, 2047 (2020)
2. A. Khayat, M. Kissaoui, L. Bahatti, A. Raihani, K. Errakkas, Y. Atifi, Microgrid short-term electrical load forecasting using machine learning models, in Proc. 4th Int. Conf. on Innovative Research in Applied Science, Engineering and Technology (IRASET), 1-7 (2024)
3. H. Guentri, T. Allaoui, M. Mekki, M. Denai, Power management and control of a photovoltaic system with hybrid battery-supercapacitor energy storage based on heuristics methods, *J. Energy Stor.* **39**, 102578 (2021)
4. J.B. Almada, R.P.S. Leão, R.F. Sampaio, G.C. Barroso, A centralized and heuristic approach for energy management of an AC microgrid, *Renew. Sustain. Energy Rev.* **60**, 1396-1404 (2016)
5. M.B. Ammar, M.A. Zdiri, R.B. Ammar, Fuzzy Logic Energy Management between Stand-alone PV Systems, *Power* **9**, 10 (2021)
6. A. Atoui, M. Seghir Boucherit, K. Benmansour, S. Barkat, A. Djerioui, A. Houari, Unified fuzzy logic controller and power management for an isolated residential hybrid PV/diesel/battery energy system, *Clean Energy* **6**, 671-681 (2022)

7. Y. Atifi, A. Raihani, M. Kissaoui, Smart Grid Production Cost Optimization by Bellman Algorithm, in Proc. Int. Conf. Smart Appl. Data Anal., 225-234 (2022).
8. H. Abdellatif, M.N. Syed, M.I. Hossain, M.A. Abido, Standalone Hybrid Renewable Energy System Optimization Using Linear Programming, Arab. J. Sci. Eng. **48**, 6361-6376 (2023)
9. H. Tian, K. Wang, B. Yu, C. Song, K. Jermsittiparsert, Hybrid improved Sparrow Search Algorithm and sequential quadratic programming for solving the cost minimization of a hybrid photovoltaic, diesel generator, and battery energy storage system, Energy Sources Part A: Recovery Util. Environ. Eff. 1-17 (2021)
10. M.A. Mosa, A.A. Ali, Energy management system of low voltage dc microgrid using mixed-integer nonlinear programming and a global optimization technique, Electr. Power Syst. Res. **192**, 106971 (2021)
11. Y. Atifi, A. Raihani, M. Kissaoui, R. Lajouad, K. Errakkas, Nonlinear control of three level NPC inverter used in PV/grid system: comparison of topologies and control methods, Bull. Electr. Eng. Inf. **13**, 2165-2174 (2024)
12. Y. Atifi, M. Kissaoui, A. Raihani, K. Errakkas, A. Khayat, Advanced Nonlinear Control of WEC System in AC Microgrid Connected to the Main Grid With Electric Vehicle Integration, e-Prime Adv. Electr. Eng. Electron. Energy, 100718 (2024)
13. Y. Huangfu, C. Tian, S. Zhuo, L. Xu, P. Li, S. Quan, Y. Zhang, R. Ma, An optimal energy management strategy with subsection bi-objective optimization dynamic programming for photovoltaic/battery/hydrogen hybrid energy system, Int. J. Hydrog. Energy **48**, 3154-3170 (2023)
14. C. Bordons, F. Garcia-Torres, M.A. Ridao, *Model predictive control of microgrids*, **358** (Springer, Berlin/Heidelberg, Germany, 2020)
15. D. Bernardini, A. Bemporad, Scenario-based model predictive control of stochastic constrained linear systems, in Proc. 48th IEEE Conf. Decis. Control (CDC) held jointly with 28th Chinese Control Conf., 6333-6338 (2009)
16. L. Valverde, F. Rosa, A.J. Del Real, A. Arce, C. Bordons, Modeling, simulation and experimental set-up of a renewable hydrogen-based domestic microgrid, Int. J. Hydrog. Energy **38**, 11672-11684 (2013)
17. P. Velarde, L. Valverde, J.M. Maestre, C. Ocampo-Martínez, C. Bordons, On the comparison of stochastic model predictive control strategies applied to a hydrogen-based microgrid, J. Power Sources **343**, 161-173 (2017)
18. Y. Atifi, A. Raihani, M. Kissaoui, M. Hajjaj, A. Bouaaddi, Towards a smart photovoltaic panel: Numerical and experimental study, in Proc. Int. Conf. Artif. Intell. Smart Environ., 788-793 (2022)